JVIN Journal of Vascular and Interventional Neurology
OFFICIAL JOURNAL OF THE ZEENAT QURESHI STROKE RESEARCH CENTER

Dural venous sinuses distortion and compression with supratentorial mass lesions: a mechanism for refractory intracranial hypertension?

Adnan I. Qureshi, **Mushtaq H. Qureshi**, **Shahram Majidi**, **Waqas I. Gilani**, and **Farhan Siddiq**
Zeenat Qureshi Stroke Institute, St. Cloud, MN

Abstract

Objective—To determine the effect of supratentorial intraparenchymal mass lesions of various volumes on dural venous sinuses structure and transluminal pressures.

Methods—Three set of preparations were made using adult isolated head derived from fresh human cadaver. A supratentorial intraparenchymal balloon was introduced and inflated at various volumes and effect on dural venous sinuses was assessed by serial intravascular ultrasound, computed tomographic (CT), and magnetic resonance (MR) venograms. Contrast was injected through a catheter placed in sigmoid sinus for both CT and MR venograms. Serial trasluminal pressures were measured from middle part of superior sagittal sinus in another set of experiments.

Results—At intraparenchymal balloon inflation of 90 cm^3, there was attenuation of contrast enhancement of superior sagittal sinus with compression visualized in posterior part of the sinus without any evidence of compression in the remaining sinus. At intraparenchymal balloon inflation of 180 and 210 cm^3, there was compression and obliteration of superior sagittal sinus throughout the length of the sinus. In the coronal sections, at intraparenchymal balloon inflations of 90 and 120 cm^3, compression and obliteration of the posterior part of superior sagittal sinus were visualized. In the axial images, basal veins were not visualized with intraparenchymal balloon inflation of 90 cm^3 or greater although straight sinus was visualized at all levels of inflation. Trasluminal pressure in the middle part of superior sagittal sinus demonstrated a mild increase from 0 cm H^2O to 0.4 cm H^2O and 0.5 cm H^2O with inflation of balloon to volume of 150 and 180 cm^3, respectively. There was a rapid increase in transluminal pressure from 6.8 cm H^2O to 25.6 cm H^2O as the supratentorial mass lesion increased from 180 to 200 cm^3.

Conclusions—Our experiments identified distortion and segmental and global obliteration of dural venous sinuses secondary to supratentorial mass lesion and increase in transluminal pressure with large volume lesions. The secondary involvement of dural venous sinuses may represent a mechanism for refractory intracranial hypertension.

Keywords

dural venous sinus; mass lesion, intracranial hypertension; superior sagittal sinus; transverse sinus

Introduction

Brain tissue compression and distortion has been studied extensively among patients with supratentorial mass lesions [1–3]. However, the effect of supratentorial mass lesions on dural venous sinuses, which may be more vulnerable to external distortion and compression owing to collapsible consistency, is not studied in detail. There is some evidence that supratentorial mass lesions can compress and increase pressure within dural venous sinuses. In an experimental model of intracranial hypertension [4], the secondary alteration in flow velocities within superior sagittal sinus have been documented. The secondary compression of venous sinuses in patients with idiopathic intracranial hypertension has been reported [5,6]. Increase in intracranial pressure and cerebral edema secondary to venous occlusion is a well-recognized phenomenon [7]. Therefore, it is possible that compression of dural venous sinuses can lead to malignant and progressive cerebral edema and intracranial hypertension in patients with mass lesions [8,9]. We performed this study to determine the relationship

Published May, 2014.

Address correspondence to: Zeenat Qureshi Stroke Institute, St. Cloud, MN, Phone: 320-281-5545, Fax: 320-281-5547, qureshai@gmail.com

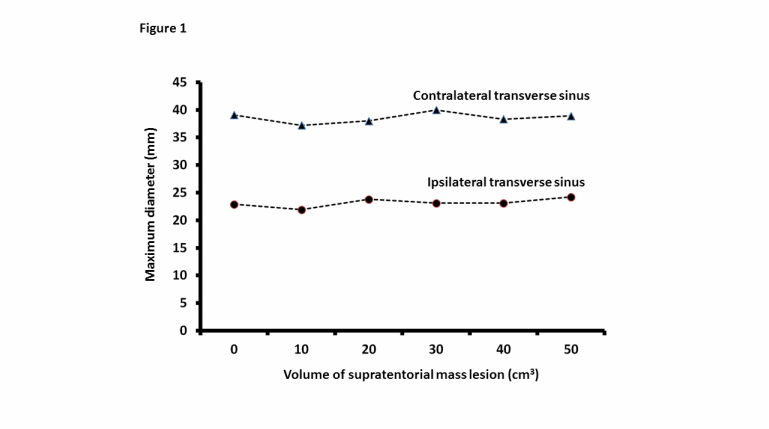

Figure 1. Maximum diameter of the ipsilateral and contralateral transverse sinuses as measured by intravascular ultrasound with various volumes of supratentorial mass lesions.

between supratentorial mass lesions of various volumes and: (1) presence and magnitude of structural change and (2) transluminal pressure changes observed within dural venous sinuses.

Methods and Results

We performed a set of studies, one focused on studying the structural effect of intracranial mass lesion on dural venous sinuses and second one focused on the change in transluminal pressure within superior sagittal sinus secondary to effect of intracranial mass lesion in a cadaveric cranium model.

Structural changes in transverse venous sinuses in response to small and moderate sized supratentorial lesions: serial intravascular ultrasound study

A preparation was made using adult isolated head derived from fresh human cadaver. The head was intact included the neck truncated at cervical sixth or seventh vertebral level. A 5-mm diameter burr hole was made after excising of skin and soft tissue to expose the skull bone. The burr right hole was made 2 cm from midline and 2 cm anterior to the Bregma. A small incision was made in dura at the site of Burr hole. A Foley's catheter was advanced through the hole into the brain tissue. The balloon of urinary catheter was inflated using contrast media and the position of balloon in the brain tissue was validated under fluoroscopy. The balloon was inflated up to 60 cm^3 with increments starting from 20 cm^3.

We cut the distal end of urinary indwelling catheter just distal to the balloon and advanced the catheter into the right jugular vein. Then we inflated the balloon of the catheter and stabilized the position of the balloon inside the jugular vein. Another urinary indwelling catheter was advanced into the left internal jugular vein and the positioned inside the jugular vein in the same fashion. Then the intravascular ultrasound (IVUS) catheter (Eagle Eye Gold, 20 MHZ Digital, 64 Bement, s5 Imaging System, Volcano Corp.) was advanced into the right internal jugular vein through the urinary indwelling catheter up to the transverse sinus under fluoroscopic guidance. IVUS images from the ipsilateral and contralateral transverse sinuses were obtained by moving IVUS probe through the whole length of both transverse sinuses. Cross-sectional real-time view were acquired after inflation of the supratentorial balloon to various volumes which included baseline, 20, 40, and 60 cm^3. Sodium chloride (0.9%) was continuously infused through the indwelling catheter from the left side to maintain the pressure inside the venous system. The IVUS images were imported to the Analyze 9.0 software (AnalzyeDirect, Inc., Overland Park, KS) to measure the maximum diameter of the contralateral and ipsilateral transverse sinuses at each of the time points. Three measurements were made for each transverse sinus and a mean value was calculated. The baseline maximum diameter of the ipsilateral and contralateral transverse sinus was 23 and 39 mm, respectively. Figure 1 demonstrates the change in diameter at each of measured time points for both ipsilateral and contralateral transverse sinus. In the presence of 50 cm^3 inflated intraparenchymal balloon, the maximum diameter of the ipsilateral and contralateral transverse sinus was 24 and 38 mm, respectively.

Journal of Vascular and Interventional Neurology

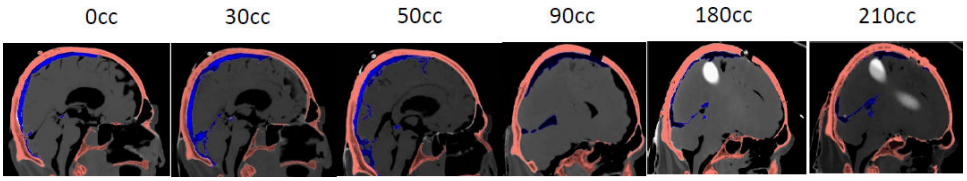

Figure 2. Serial CT venograms (sagittal section) obtained with various volumes of supratentorial mass lesions. Note the attenuation of contrast enhancement of superior sagittal sinus with compression visualized in posterior part of the sinus at intraparenchymal balloon inflation of 90 cm^3.at intraparenchymal balloon inflation of 180 and 210 cm^3, there was extensive compression and obliteration of superior sagittal sinus.

Structural changes in dural venous sinuses in response to small-, moderate-, and large-sized supratentorial lesions: serial computed tomographic venographic study

A preparation was made using adult isolated head derived from fresh human cadaver as mentioned above. A Foley's catheter was advanced through the burr hole into the brain tissue and inflated up to 60 cm^3 in increments. A custom-made balloon was made by attaching a commercially available rubber balloon with a rubber catheter for larger volume inflations. A 6 F Envoy catheter (Emerald, Cordis, NJ) was introduced into the internal jugular vein through the exposed transected cervical end. The guide catheter was advanced over a 0.035 glide wire up to the sigmoid sinus under fluoroscopic guidance (Ziehm Vista, Instrumentarium Imaging Ziehm, Inc., Riverside, CA). A continuous infusion of 0.9% sodium chloride was maintained through the guide catheter at a rate of 200 cm^3/h. Computed tomographic (CT) scans were obtained with 5-mm-thick contiguous axial, coronal, and sagittal sections from the base of the skull to the vertex, followed immediately by CT venography at eight time points. These time points were: baseline, and 20, 30, 50, 90, 120, 180, and 210 cm^3 of intraparenchymal balloon inflations. Scans were angled parallel to a line drawn from the posterior margin of the foramen magnum to the superior margin of the orbit. All CT venographies were performed on Siemnens filamtome definition flash with a 3-D workstation. The scanning parameters used were a slice thickness of 0.6 mm at an interval of 5.0 mm. The gantry rotation speed was 3.5–7.5 mm per rotation using 120 kV and 250–300 mA with a prescan delay of 30–40 s. A total of 70–80 mL of nonionic contrast material (optiray, 370 mg I/mL) was administered at a rate of 4–5 mL/s by a power injector into the sigmoid sinus. Using VITAL IMAGES computer software (Vitrea2 version 4.1.14.0) venograms were displayed using maximum intensity projection (MIP), volume averaging, and integral algorithms. The baseline sagittal CT venogram images were reviewed and image that displayed the superior sagittal sinus was selected. The coronal section CT venogram was reviewed and the image that displayed the transverse sinuses and confluence of sinuses was selected. The axial section CT venogram was reviewed and section that displayed the straight sinus, vein of Galen, and basal veins was selected. Subsequent axial, coronal, and sagittal sections images at various time points were reviewed and corresponding images were selected. In some instances, corresponding image was not available. The selected were imported to the Analyze 9.0 software (AnalzyeDirect) for postprocessing. The skull bone and contrast enhanced venous sinuses were assigned different colors based on density thresholding technique with manual correction if necessary.

In the sagittal image, the superior sagittal sinus was well visualized in images acquired with intraparenchymal balloon inflation of 30 and 50 cm^3 (Figure 2). At intraparenchymal balloon inflation of 90 cm^3, there was attenuation of contrast enhancement of superior sagittal sinus with compression visualized in posterior part of the sinus without any evidence of compression in the remaining sinus. At intraparenchymal balloon inflation of 180 and 210 cm^3, there was compression and obliteration of superior sagittal sinus throughout the length of the sinus. In the coronal sections (Figure 3), the transverse sinuses and confluence of sinuses appeared patent with 20, 30, and 50 cm^3 of intraparenchymal balloon inflation. At intraparenchymal balloon inflations of 90 and 120 cm^3, compression and obliteration of the posterior part of superior sagittal sinus was visualized. At intraparenchymal balloon inflations of 210 cm^3, compression of ipsilateral transverse sinus was visualized with complete obliteration of superior sagittal sinus. In the axial images (Figure 4), straight sinus, vein of Galen, and basal veins were visualized with 20, 30, and 50 cm^3 of intraparenchymal balloon inflation. Basal veins were

Journal of Vascular and Interventional Neurology

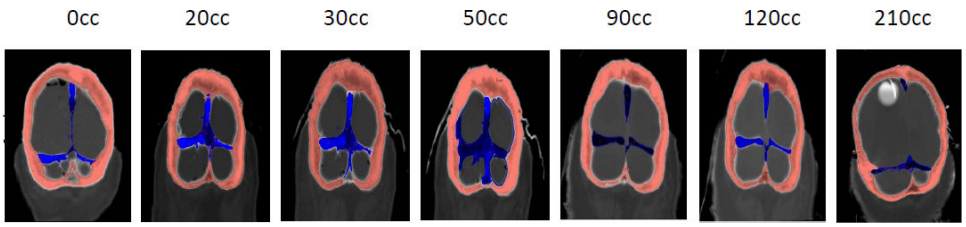

Figure 3. Serial CT venograms (coronal section) obtained with various volumes of supratentorial mass lesions. Note the compression and obliteration of the posterior part of superior sagittal sinus with intraparenchymal balloon inflations of 90 and 120 cm^3. Note the compression of ipsilateral transverse sinus and complete obliteration of superior sagittal sinus intraparenchymal balloon inflations of 210 cm^3.

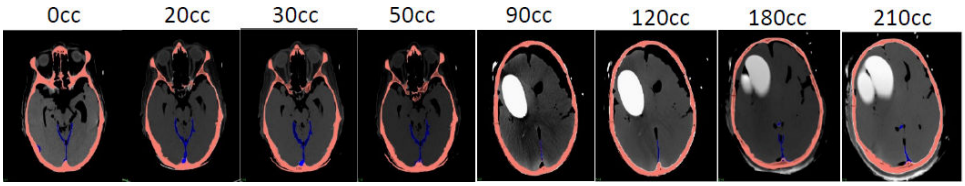

Figure 4. Serial CT venograms (axial section) obtained with various volumes of supratentorial mass lesions. Note that basal veins were not visualized with 90, 120, 150, and 210 cm^3 of intraparenchymal balloon inflation.

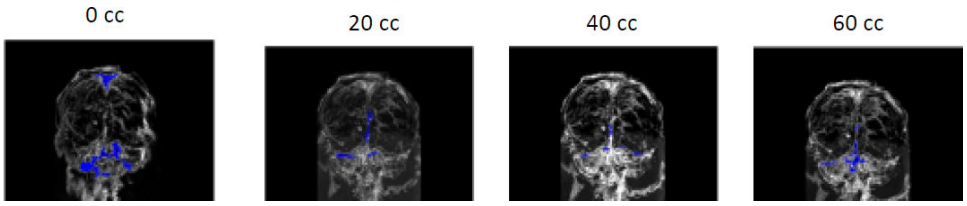

Figure 5. Serial MR venograms (coronal section) obtained with various volumes of supratentorial mass lesions.

not visualized with 90, 120, 150, and 210 cm^3 of intraparenchymal balloon inflation although straight sinus was visualized at all levels of inflation.

Structural changes in dural venous sinuses in response to small- and moderate-sized supratentorial lesions: serial magnetic resonance (MR) venographic study

Another set of experiments was performed using a similar setup and serial MR venograms were obtained. All MR venography was performed on a 1.5-T MRI system (Vision, Siemens Medical Solutions) at four time points. These time points were: baseline, and 20, 40, and 60 cm^3 of intracranial balloon inflation. Preliminary MRI of the brain was performed using the T1-weighted sequence (axial, sagittal, and coronal planes). Our parameters were slice thickness, 1.5–3.0 mm; and matrix size, 144 × 256. The total number of acquisitions was 1 or 2, and the total acquisition time was 6–8 min. After the acquisition of all source images of the MR venography sequence, the images were processed and displayed by means of an MIP algorithm using computer software.

In the sagittal image, the superior sagittal sinus was well visualized in images acquired with intraparenchymal balloon inflation of 20, 40, and 60 cm^3 (not shown). In the coronal images (Figure 5), there was some evidence of distortion of the superior sagittal sinus with 20, 40, and 60 cm^3 of intraparenchymal balloon inflation. In the axial images (not shown), straight sinus, vein of Galen, and basal veins were visualized with 20, 40, and 60 cm^3 of intraparenchymal balloon inflation.

We did not perform MR venogram in the second set of experiments with large mass lesions because the data

Journal of Vascular and Interventional Neurology

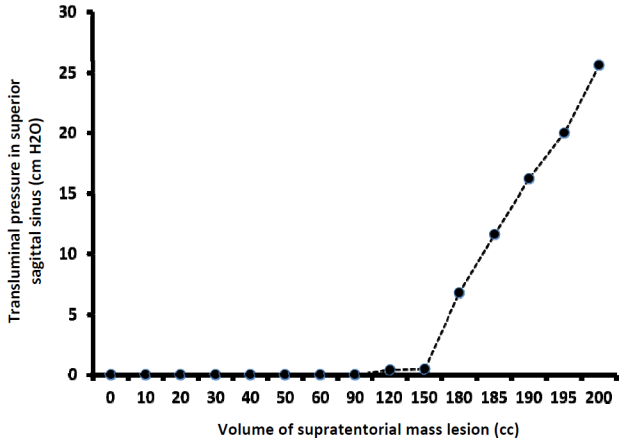

Figure 6. The superior sagittal sinus transluminal pressure measurements at baseline and at various volumes of supratentorial mass lesions.

provided by CT venogram was of higher quality than MR venogram in the first set of experiments.

Transluminal pressure changes in dural venous sinuses in response to small-, moderate-, and large-sized supratentorial lesions: serial fluid-coupled transducer study

A similar setup as mentioned above was prepared. A second craniotomy hole was created in the midline above the posterior aspect of the superior sagittal sinus 3 cm posterior to Bregma. The surface of the superior sagittal sinus was exposed and a small incision was made. A 2.3 F microcatheter with a latex balloon mounted on the tip was introduced and advanced in anterior direction under fluoroscopic guidance using C arm unit (Ziehm Vista, Instrumentarium Imaging Ziehm, Inc.). The microcatheter was placed in mid position of the superior sagittal sinus. The balloon was filled with fluid, and the pressure was transmitted through the catheter and measured with an external fluid column similar to the setup used in pressure measurements during lumbar puncture. The balloon was inflated using contrast (Omnipaque 140) diluted in 0.9% sodium chloride solution under fluoroscopic guidance to avoid deformation of balloon or sinus. Using the balloon technique, a pressure is measured that is the average pressure along the balloon and in various radial directions. The superior sagittal sinus pressure was measured at baseline, and 10, 20, 30, 40, 50, and 60 cm^3 of intraparechymal balloon inflations. The intraparenchymal balloon was replaced by larger custom made balloon. The superior sagittal sinus pressure was measured at baseline, and at 90, 120, 150, 180, 185, 190, 195, and 200 cm^3 of intraparechymal balloon inflations.

There was no change in trasluminal pressure in the middle part of superior sagittal sinus up to 90 cm^3 inflation of intraparenchymal balloon. Trasluminal pressure in the middle part of superior sagittal sinus demonstrated a value of 0.4 cm H^2O and 0.5 cm H^2O with inflation of balloon to volume of 150 and 180 cm^3, respectively. There was a rapid increase in transluminal pressure from 6.8 cm H^2O to 25.6 cm H^2O as the supratentorial mass lesion increased from 180 to 200 cm^3 (see Figure 6).

Exploratory clinical studies

We identified all acute ischemic stroke patients at a University affiliated hospital that records demographic and pertinent clinical data regarding all patients discharged with a diagnosis of stroke. We identified patients with fatal middle cerebral artery infarction due to malignant cerebral edema who were admitted between 2008 and 2010 who had undergone a MRI of the brain at least 3 days after symptom onset using an institutional registry. Among the 196 patients admitted with ischemic stroke, 14 developed fatal cerebral edema during their hospitalization. Out of this population subset, only three patients met the criteria of having MRI scans with both coronal and sagittal views available at least 3 days after symptom onset. Among these three patients, two had radiological evidence of compression of superior sagittal sinuses. The MRI revealed an extremely large infarction affecting the right or left middle cerebral arteries with midline shift and evidence of cingulate and uncal hernia-

Journal of Vascular and Interventional Neurology

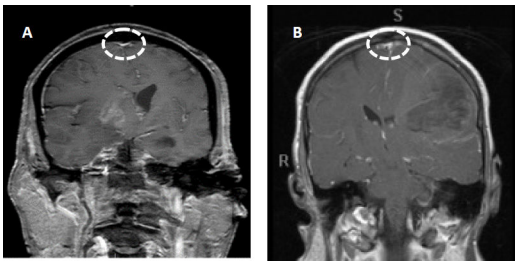

Figure 7. Two representative cases of compression of superior sagittal sinus (encircled) due to large middle cerebral artery infarction.

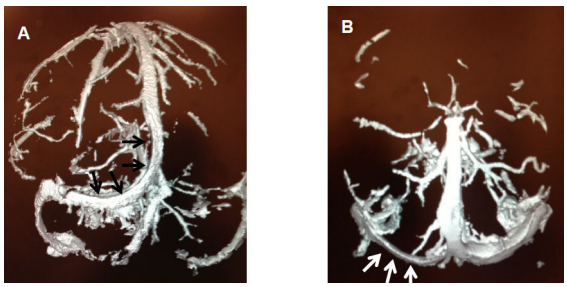

Figure 8. Two representative cases of compression of transverse sinus due to large middle cerebral artery infarctions; the arrows identify the segments of venous sinuses that are either compressed or displaced.

tion (see Figure 7). There was compression and near obliteration of the superior sagittal sinus on the coronal sections of the MRI in both patients (see Figure 7).

We prospectively identified four consecutive patients with supratentorial mass lesions who underwent a CT perfusion or angiogram within a 2-month as part of routine care. Multiple axial images performed through the brain with intravenous contrast using standard perfusion CT technique. Three-dimensional reconstructions and dynamic evaluation and dynamic enhancement of the cerebral dural venous sinuses were performed using a Vitrea® workstation equipped with brain perfusion package. The patients' demographic and clinical data with CT venographic findings were as follows: 82-year-old man with large temporal hemorrhage (displacement of transverse sinus and posterior part of superior sagittal sinus); 88-year-old woman with large middle cerebral artery ischemic stroke (downward displacement of transverse sinus with compression, Figure 8A); 80-year-old woman with large temporo-occipital hemorrhage (displacement of posterior part of superior sagittal sinus); and 82-year-old man with large middle cerebral artery ischemic stroke (compression of transverse sinus, Figure 8B). The findings are preliminary and subject to limitations imposed by image acquisition and reconstruction, and variations in venous anatomy.

Discussion

Our experiments demonstrate compression of dural venous sinus secondary to supratentorial mass lesion and increase in transluminal pressure with large volume lesions. Compression of dural venous sinuses with increase in transluminal pressure can lead to venous engorgement and reduced venous outflow. Therefore, secondary or possibly a propagating cascade of increasing intracranial pressure and cerebral edema can be initiated through such a mechanism. We observed four stages of dural venous sinuses involvement with increasing volume of intraparenchymal balloon inflation. The first stage (distortion stage) was seen with intraparenchymal balloon inflation of less than 90 cm^3 and consisted of flattening and distortion of the superior sagittal sinus and noticeable displacement of straight sinus. The second stage (segmental obliteration) was seen with intraparenchymal balloon inflation of ranging between 90 and 150 cm^3 and consisted of obliteration of posterior part of sagittal sinus and basal veins. The third stage (global obliteration) was seen with intraparenchymal balloon inflation of ranging above 150 cm^3 and consisted of obliteration of the superior sagittal sinus with rapid increase in transluminal pressure and compression of ipsilateral transverse sinus.

Journal of Vascular and Interventional Neurology

Journal of Vascular and Interventional Neurology

The effects of supratentorial mass lesions are likely to be underestimated in cadaveric cranium model. Postmortem brain volume loss may allow greater accommodation of mass lesions without effecting cranial structures [10,11] than that expected in alive patients. The compression of dural venous sinuses maybe more in the presence of expanded state owing to continuous blood flow. The artifact created because of repeated contrast injection even with a circulating circuit may obscure some of the findings on serial CT and MR venograms. While the exact quantitation of effect on dural venous sinuses maybe limited by the inherent limitations of our protocol, the model provided information regarding presence and characteristics of such effects. The functional impact of compression of superior sagittal and transverse sinuses has to be interpreted with the understanding that both superficial and deep middle cerebral veins can drain into the cavernous and laterocavernous sinuses [12–14]. Therefore, an alternate route for venous drainage may be activated reducing or ameliorating the physiologic effect of venous compression of selected sinuses.

Hyperemic regions with a loss of auto regulation are seen in sites remote from the supratentorial mass lesions without a clear etiology [15–17]. Our experiments suggests that venous stasis in territories drained by superior sagittal sinus may be a potential mechanism for remote hyperemia. Similarly, the etiology of minute brainstem hemorrhage and hypodensities by rapidly increasing intracranial pressure and herniation is debated [18,19]. Stretching and laceration of pontine perforating branches of the basilar artery and venous thrombosis and infarction have been proposed as explanations [20]. Hyperperfusion in the thalamus and the midbrain in an experimental model of unilateral compressive lesion and transtentorial herniation support the concept of venous compression [21]. The diencephalon and rostral brain stem are supplied by great vein of Galen and the basal veins both of which are vulnerable to compression from swelling or displacement of the midbrain due to supratentorial mass lesion [22]. We noted in our experiments that basal veins were not visualized with large mass lesions which would support the notion of venous compression as an etiology for midbrain hemorrhages.

The practical implications of dural venous sinus compression and distortion remain undefined. It remains unclear whether incremental increase in intracranial pressure and cerebral edema is more or less likely to respond to treatments such as mannitol and hypertonic saline. The rheological effect of mannitol and hypertonic saline may be advantageous in alteration in venous flow in presence of mass lesion [23]. The hemodilution secondary to increase in intravascular osmolality and subsequent movement of fluids into the intravascular compartment may limit the magnitude of flow alterations. Further studies will be required to determine the occurrence of such phenomenon in various supratentorial mass lesions and whether such phenomenon is modifiable with therapeutic interventions.

Acknowledgements and Funding

This study was performed independently of any financial support. None of the authors have any conflict of interest to disclose and there are no financial conflicts to disclose.

Dr. Qureshi has received funding from National Institutes of Health U01-NS062091-01A2 (medication provided by EKR Therapeutics), American Heart Association Established Investigator Award 0840053N, and the Minnesota Medical Foundation, Minneapolis, MN, USA

References

1. Yang H, Chopp M, Jiang F, Zhang X, Schallert T. 2006;Interruption of functional recovery by the nmda glutamate antagonist mk801 after compression of the sensorimotor cortex: Implications for treatment of tumors or other mass-related brain injuries. *Experimental Neurology* 200:262–6.
2. Burger R, Bendszus M, Vince GH, Solymosi L, Roosen K. 2004Neurophysiological monitoring, magnetic resonance imaging, and histological assays confirm the beneficial effects of moderate hypothermia after epidural focal mass lesion development in rodents. *Neurosurgery* . 54 :701–711. 711–02.discussion
3. Toyota S, Graf R, Dohmen C, et al. 2001Elevation of extracellular glutamate in the final, ischemic stage of progressive epidural mass lesion in cats. *Journal of Neurotrauma* 18. :1349–57.
4. Anile C, De Bonis P, Fernandez E, et al. 2012;Blood flow velocities during experimental intracranial hypertension in pigs. *Neurological Research* 34:859–63.
5. Rohr A, Bindeballe J, Riedel C, van Baalen A, Bartsch T, Doerner L, et al. The entire dural sinus tree is compressed in patients with idiopathic intracranial hypertension: a longitudinal, volumetric magnetic resonance imaging study. *Neuroradiology* 2012;54:25–33.
6. Stienen A, Weinzierl M, Ludolph A, Tibussek D, Hausler M. 2008;Obstruction of cerebral venous sinus secondary to idiopathic intracranial hypertension. *European Journal of Neurology : The Official Journal of the European Federation of Neurological Societies* 15:1416–8.
7. Saposnik G, Barinagarrementeria F, Brown RD Jr, et al. 2011;Diagnosis and management of cerebral venous thrombosis: a statement for healthcare professionals from the american heart association/ american stroke association. *Stroke; a Journal of Cerebral Circulation* 42:1158–92.
8. Higgins JN, Burnet NG, Schwindack CF, Waters A. 2008;Severe brain edema caused by a meningioma obstructing cerebral venous outflow and treated with venous sinus stenting. Case report. *Journal of Neurosurgery* 108:372–6.

9. Czernicki Z, Grochowski W, Uchman G, Tychmanowicz K, Razumowski AE. 1991;[Occlusion of the superior sagittal sinus caused by meningioma, intracranial volume-pressure relations and brain edema]. *Neurologia i neurochirurgia polska* 25:580–6.
10. Harvey FH. 1980;The significance of the amount of fluid surrounding the brain to the recognition of brain swelling (or atrophy) at autopsy: a new and routinely applicable method of diagnosing abnormal brain size. *Journal of Forensic Sciences* 25:287–96.
11. Maxeiner H, Behnke M. 2008;Intracranial volume, brain volume, reserve volume and morphological signs of increased intracranial pressure–a post-mortem analysis. *Legal Medicine* 10:293–300.
12. Andeweg J. 1996;The anatomy of collateral venous flow from the brain and its value in aetiological interpretation of intracranial pathology. *Neuroradiology* 38:621–8.
13. Nagata T, Ishibashi K, Metwally H, et al. 2013;Analysis of venous drainage from sylvian veins in clinoidal meningiomas. *World Neurosurgery* 79:116–23.
14. Gailloud P, San Millan Ruiz D, Muster M, Murphy KJ, Fasel JH, Rufenacht DA. 2000;Angiographic anatomy of the laterocavernous sinus. *American Journal of Neuroradiology* 21:1923–9.
15. Endo H, Larsen B, Lassen NA. 1977;Regional cerebral blood flow alterations remote from the site of intracranial tumors. *Journal of Neurosurgery* 46:271–81.
16. Kuroda K, Skyhoj Olsen T, Lassen NA. 1982;Regional cerebral blood flow in various types of brain tumor. Effect of the space-occupying lesion on blood flow in brain tissue close to and remote from tumor site. *Acta Neurologica Scandinavica* 66:160–71.
17. Olsen TS, Larsen B, Skriver EB, Herning M, Enevoldsen E, Lassen NA. 1981;Focal cerebral hyperemia in acute stroke. Incidence, pathophysiology and clinical significance. *Stroke; A Journal of Cerebral Circulation* 12:598–607.
18. Alexander E Jr, Kushner J, Six EG. 1982;Brainstem hemorrhages and increased intracranial pressure: from duret to computed tomography. *Surgical Neurology* 17:107–10.
19. Qureshi AI, Geocadin RG, Suarez JI, Ulatowski JA. 2000;Long-term outcome after medical reversal of transtentorial herniation in patients with supratentorial mass lesions. *Critical Care Medicine* 28:1556–64.
20. Parizel PM, Makkat S, Jorens PG, et al. 2002;Brainstem hemorrhage in descending transtentorial herniation (duret hemorrhage). *Intensive Care Medicine* 28:85–8.
21. Zierski J. 1987;Blood flow in brain structures during increased ICP. *Acta Neurochirurgica. Supplementum* 40:95–116.
22. Andeweg J. 1999;Consequences of the anatomy of deep venous outflow from the brain. *Neuroradiology* 41:233–41.
23. Qureshi AI, Suarez JI. 2000;Use of hypertonic saline solutions in treatment of cerebral edema and intracranial hypertension. *Critical Care Medicine* 28:3301–13.

Journal of Vascular and Interventional Neurology